PHYSICAL REVIEW B VOLUME 62, NUMBER 8 15 AUGUST 2000-II

Structure and electronic properties of potassium-doped single-wall carbon nanotubes

A. S. Claye,[1,3] N. M. Nemes,[2,3] A. Jánossy,[4] and J. E. Fischer[1,3,*]
[1]*Department of Materials Science and Engineering, University of Pennsylvania, Philadelphia, Pennsylvania 19104-6272*
[2]*Department of Physics and Astronomy, University of Pennsylvania, Philadelphia, Pennsylvania 19104-6396*
[3]*Laboratory for the Research on the Structure of Matter, University of Pennsylvania, Philadelphia, Pennsylvania 19104-6272*
[4]*Technical University of Budapest, Institute of Physics, P.O. Box 91, H-1521 Budapest, Hungary*
(Received 3 May 2000)

The structure and electronic properties of potassium-doped single-wall carbon nanotubes have been studied by conduction electron spin resonance, conductivity (σ), and x-ray diffraction (XRD), using *in situ* electrochemical methods. The spin susceptibility χ_P of the K-saturated phase is independent of temperature; a lower bound is 5×10^{-8} emu/g. At 300 K both σ and χ_P increase monotonically and reversibly with K/C. The spin relaxation rate and g factor do not change with doping, and XRD reveals an irreversible loss of crystallinity upon doping. We propose an inhomogeneous doping model to explain these results.

The electronic properties of alkali doped single-wall carbon nanotubes (SWNT) exhibit dramatic changes with respect to the undoped material. Vapor phase potassium doping decreases the 300 K resistivity by a factor of 30.[1,2] Electron transfer was inferred from doping-induced redshifts of intratube Raman-active modes.[3] Reversibility of the doping process has yet to be demonstrated. The structure of doped material, and the degree of long-range order, remains controversial. Models have been proposed assuming an ordered superlattice,[4] while most experiments show that alkali doping disrupts the rope structure.[5–9]

In principle conduction electron spin resonance (CESR) can probe the doping dependence of the electronic structure. The temperature-independent Pauli paramagnetism of conduction electrons is a signature of metallicity, and χ_P is a direct measure of the density of states at the Fermi energy $N(E_F)$. Also, comparison of the temperature (T) and doping dependences of the CESR linewidth (proportional to the spin relaxation rate) with the momentum relaxation rate (proportional to resistivity) can reveal non-Fermi-liquid and/or reduced dimensionality effects.[10] CESR was observed in undoped SWNT by Petit *et al.*[11] but not by Bandow *et al.*;[12] and was recently reported in K-doped SWNT at fixed concentration.[13]

Electrochemistry is a powerful doping method because it affords precise control of guest concentration, facilitates *in situ* experiments on air-sensitive materials, and provides a controlled method to test reversibility. Examples include CESR of doped polyacetylene $[(CH)K_y]_x$ vs y,[14] and x-ray diffusion (XRD) of Li-doped SWNT.[7,8] Here we use electrochemical doping and *in situ* CESR, σ, and XRD to elucidate the structural and electronic properties of K-doped SWNT. Our samples were in the form of highly purified, $\sim50\,\mu$m thick ''buckypaper.''[15] Grade I had no detectable graphite or amorphous carbon and little nickel by XRD,[16] while grade II contained $\sim5\%$ graphite and ~5 times more nickel than grade I. Below we show how the impurities turned out to be very useful, without affecting our conclusions. Electrochemical cycling was carried out with a small fixed current to ensure equilibrium conditions for physical measurements, using 1M KCN in anhydrous $(C_2H_5)_3B$/THF electrolyte.[14] Cyclic voltammetry on separate samples confirmed that the graphite in grade II contributes negligibly to the total K uptake. With this scheme the saturation value of K/C is 1/24 rather than $\sim1/8$ with vapor doping,[1] the same two values that are found with graphite as host. Vapor-doped KC_8-graphite is a stage 1 binary compound in which all sites are occupied. The electrochemically doped version is a stage 1 *ternary* compound $K(THF)_{2.5}C_{24}$ in which THF partially solvates the transferred electron and thereby occupies a volume equivalent to $\sim2/3$ of the sites.[17,18] The fact that we find the same two K/C ratios in SWNT suggests that both the charge-transfer/steric limits per carbon (vapor doping), and solvation effects (electrochemical doping) are about the same in both hosts.

The *in situ* ESR cell consisted of a 4 mm diam quartz tube, a Kovar/pyrex graded seal, and a Swagelok compression fitting with a teflon plug for the two electrode leads. The sample was contacted with Pt, and the K counterelectrode was 4 cm above the sample to avoid perturbing the cavity. *Ex situ* samples for *T*-dependent CESR measurements were doped to saturation and sealed in quartz after evacuation and backfilling with 50 mtorr He for heat transfer. Absolute susceptibilities were referenced to $CuSO_4\cdot5H_2O$. Four-probe *in situ* σ and XRD were measured as described previously.[7] Constant-current doping/dedoping was interrupted at intervals to accumulate XRD profiles for several hours. All manipulations were carried out in a circulating Ar glove box.

Figure 1 shows the evolution of ESR spectra with the K/C ratio. Two signals are observed: a broad ferromagnetic resonance (FMR) from the Ni and a narrow line which we identify as CESR in doped SWNT. The microwave skin effect alters the line shapes of both as doping proceeds. If the sample thickness t is comparable to or larger than the skin depth δ, the phase of the exciting field is inhomogeneous and a mixture of absorption and dispersion is detected. Defining this ratio as $R=\tan(\phi)$, the phase of the detected signal varies between the limits $\phi=0$ ($t\ll\delta$) and $\phi=\pi/4$ (a 1:1 ratio of absorption and dispersion) for $\delta\ll t$.[19] Kramers-Kronig transforms were performed to obtain the doping dependence of phase and intensity for both resonances.

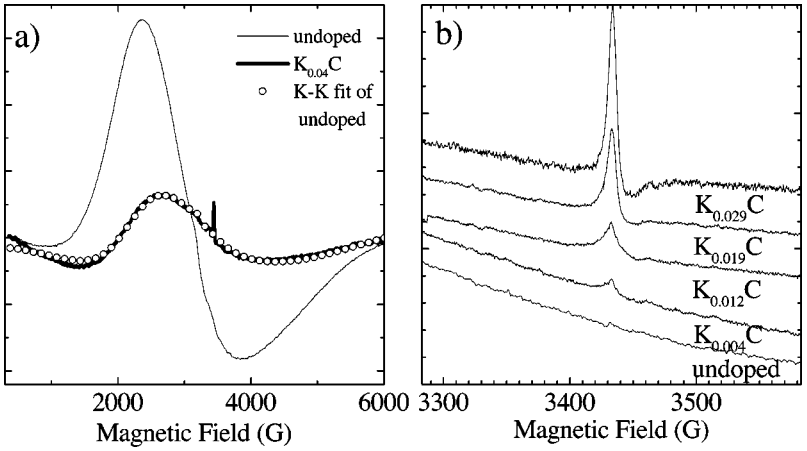

FIG. 1. (a) Ferromagnetic resonance of Ni catalyst particles in the undoped and fully doped SWNT (light and heavy curves, respectively). A linear superposition of the undoped spectrum and its Kramers-Kronig transform (open circles) fits the doped line very well. The narrow CESR line is visible at $g=2.002$ in the doped spectrum. (b) The CESR line grows continuously with increasing K concentration; the susceptibility (proportional to the amplitude) increases monotonically while the spin relaxation rate (width) and g factor (position) remain constant. The spectra as presented are not corrected for the skin effect (see text).

Ni particles are not affected by doping and are much smaller than δ, so we used the FMR to determine δ/t and the corresponding phase change with doping. Figure 1(a) shows that after saturation doping to K/C$=0.04$, the FMR is well fit by a linear combination of the undoped spectrum and its K-K transform, yielding the doping dependence of the phase and intensity. The intensity decreases monotonically with K/C, consistent with a continuous decrease in δ; σ increases with doping, and the fraction of Ni particles excited by the microwave field decreases. The maximum phase change upon doping is 46° suggesting that $\delta>t$ in the undoped sample and $\delta<t$ after saturation doping. We determined δ(K/C) from the complex impedance by fitting the FMR intensity and phase. The resulting microwave σ is plotted vs K/C in Fig. 2(a), normalized to the undoped value. Assuming $\delta=t=50\,\mu$m for the undoped sample, then $\sigma_{\mu w}\sim 100/(\Omega\,\mathrm{cm})$. The solid curve shows the *in-situ* four-probe σ(K/C) from a different sample, for which the directly, measured undoped value σ_{DC} is also $\sim 100/(\Omega\,\mathrm{cm})$. Both measurements exhibit a continuous increase in σ upon doping, which is fully reversible upon dedoping. The maximum σ enhancement at 300 K is a factor of 15 for KC_{24}, half that reported for vapor-doped SWNT-KC_8.[1,20]

Next we discuss the *in situ* CESR signal and its evolution with doping. No CESR was observed in undoped material. A well-defined line emerged with increasing K/C, while its linewidth and g factor did not change, as shown in Fig. 1(b). The CESR intensity increased continuously with doping, and the K-K phase of the CESR and FMR lines evolved together. The δ-corrected χ_P was obtained by multiplying the integrated CESR intensity by the amplitude ratio of the K-K transformed FMR in the undoped and doped states. Figure 2(b) shows that χ_P increases monotonically with K/C and is fully reversible upon dedoping. The slope of χ_P vs K/C is not constant; two inflection points can be observed at K/C $=0.007$ and 0.02. These two values coincide with features in the doping dependence of the Raman spectra for K-doped SWNT. In Fig. 2(c) we present the tangential mode shift of K-doped SWNT, measured *in situ* vs K/C.[21] Above K/C $=0.007$, a continuous (and reversible) downshift is observed due to charge-transfer-induced softening of the C-C bonds,[3] consistent with the concomitant increases in σ and χ_P. At lower K/C the shift is not monotonic, precisely in the range where χ_P depends only weakly on K/C. We tentatively ascribe this regime to metallization of semiconducting tubes in the sample.

The absence of CESR in undoped material is surprising since $\sim 1/3$ of the tubes in bulk SWNT are believed to be intrinsically metallic. Also unusual is the independence of the CESR linewidth on K/C. The usual mechanism for relaxational broadening in guest-host systems is spin-orbit scattering on the dopants, which increases strongly with atomic number and depends sensitively on the electronic structure. If the doping were homogeneous, the linewidth would increase with increasing K concentration. Anticipating the XRD results presented below, we propose a two-phase model of K-saturated domains embedded in undoped regions in order to account for the K/C–independent linewidth. The CESR is, in principle, a coupled resonance of undoped and

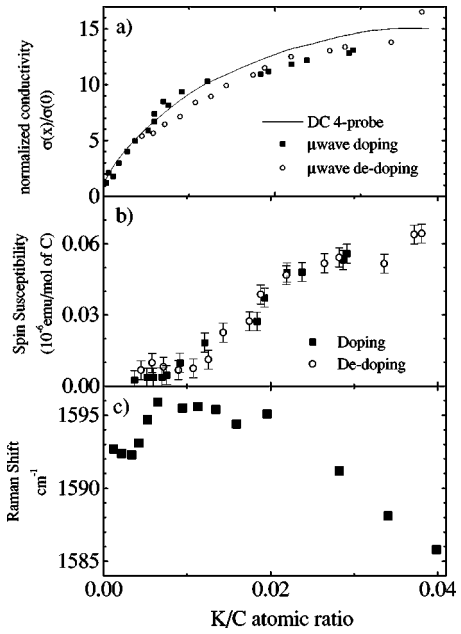

FIG. 2. (a) Electrical conductivity increases monotonically with K doping; four-probe dc (solid curve) and microwave results (filled and empty symbols for doping and dedoping respectively) change similarly and reversibly. Microwave conductivity is obtained by analyzing the skin effect. (b) Spin susceptibility also evolves reversibly with K concentration; the slope change near K/C$=0.007$ is statistically significant (see text). Results are volume-corrected to account for the K/C–dependent skin depth. (c) The Raman shift of the SWNT tangential modes also evolves continuously (and reversibly; not shown) with doping. Nonmonotonic behavior is observed for K/C<0.007.

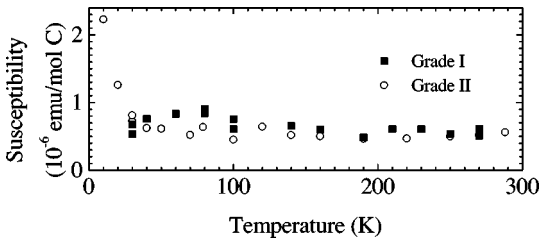

FIG. 3. Susceptibility vs T for saturation-doped SWNT, K/C $=0.04$. χ is independent of T above ~ 50 K, characteristic of a metal, and is independent of graphite impurity concentration.

doped regions. However, if the DOS and thus χ_P is much larger in the doped regions, they will dominate the observed resonance even at small K/C ratios. The homogeneous linewidth is proportional to $1/T_1=(\chi_u V_u/T_{1u}+\chi_d V_d/T_{1d})/(\chi_u V_u+\chi_d V_d)$, where $\chi_{u(d)}$, $V_{u(d)}$, $T_{1u(d)}$ are the susceptibility, volume, and lifetime of undoped (doped) regions. Inhomogeneous doping increases the number and/or size of K-saturated domains without changing their electronic structure; thus T_1 is independent of the *global* K/C ratio except at very low concentrations.

We do not observe the CESR of undoped metallic nanotubes. This is unexpected since carbon is a light element and the spin lifetime should be very long. However, spin relaxation may be dominated by Ni particles. In pure nanotubes the momentum scattering time τ is long, and the spin diffusion length $\delta_{\text{spin}}=\sqrt{v_F^2 T_1 \tau}$ is several μm, i.e., longer than the average distance electrons travel to reach a Ni particle. In this case the CESR is strongly broadened by coupling to the FMR.[22] At higher K concentrations both T_1 and τ become shorter and the CESR is decoupled from the FMR since most spins relax within the nanotubes before reaching a Ni particle.

Figure 3 presents χ_P(T) for grade I and II samples doped to saturation. χ_P is independent of T above 50 K for both samples, characteristic of a metal. Its absolute value is $\sim 5\times 10^{-8}$ emu/g (close to that reported for K-doped multiwall tubes[23]), from which $N(E_F)\approx 0.015$ states/eV·C·spin. This value is ~ 5 times smaller than a theoretical estimate [24] for tubes with an appropriate diameter distribution[15] uniformly doped with $1e^-$ per 24 C. This discrepancy may be due in part to solvation effects, i.e., less than one delocalized electron per K. We can rule out significant contribution to χ from doping the graphite impurities. First, χ is about the same for two samples with widely different graphite concentrations. Second, χ_P for *pure* $K(THF)_{2.5}C_{24}$ is less than 4×10^{-8} emu/g,[17] so 5% doped graphite impurity would account for at most 4% of our measured χ. Finally the linewidth in the graphite ternary is less than 1 G (Ref. 17) as opposed to the ~ 15 G we observe here.

Figure 4 presents a series of *in situ* XRD profiles for K-doped SWNT, as the working electrode (grade II) is taken through one full cycle. In the undoped spectrum, the broad peak at $0.42\,\text{Å}^{-1}$ is the (10) reflection of the two-dimensional (2D) triangular lattice, while the sharp peak at $1.87\,\text{Å}^{-1}$ is the graphite (002) reflection. The shoulder on the low-Q side of graphite (002) is attributed to graphitic onions, with intershell spacings slightly larger than the 3.357 Å ideal graphite value. Higher order reflections of the 2D lattice are obscured by strong scattering from the electrolyte,

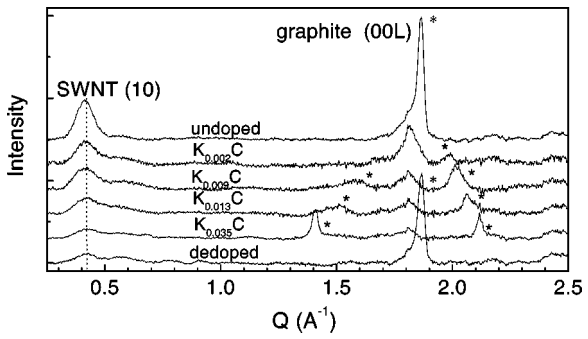

FIG. 4. *In situ* XRD profiles as a function of doping level. The (10) reflection from the 2D SWNT lattice ($0.42\,\text{Å}^{-1}$) loses intensity continuously and irreversibly, but does not shift, with increasing K/C ratio. Peaks associated with reversible staging transitions in the ternary K/THF/graphite system are labeled by (*); these originate in the $\sim 5\%$ graphite impurity content (grade II, see text).

which has been subtracted from the plotted profiles. Upon doping, we observed a gradual intensity loss of the 2D (10) reflection without any measurable shift in position. This intensity loss was irreversible, as seen in the bottom spectrum for the fully dedoped sample. At the same time the graphite (002) intensity decreases and new peaks (*) emerge. These can all be indexed as (00L) reflections from stages 1–4 K/THF/graphite ternaries.[18] These disappear upon dedoping, and the graphite (002) is recovered, confirming that K intercalation in graphite is entirely reversible and that the cell functioned properly. On the contrary, the SWNT (10) reflection was not recovered, suggesting that K insertion introduces irreversible structural disorder in the 2D rope lattice. This effect has been observed before from *in situ* XRD of Li-doped SWNT (Ref. 7) and TEM and XRD studies of SWNT exposed to K vapor,[5,6] all of which showed a crystallinity loss upon doping. It also implies that K ions, perhaps solvated by THF, invade the van der Waals spacings between adjacent tubes in a rope, but in a disordered fashion which precludes the existence of intercalation superlattices. The fact that the (10) intensity decreases but does not shift with increasing K/C is consistent with the inhomogeneous doping picture. The continuous but incomplete intensity loss suggests that some regions are fully doped and noncrystalline, while some others are not doped and retain the pristine crystal structure. Two-phase behavior was not observed in the Raman spectra, most likely because the linewidth increased with doping such that any unshifted contribution from undoped domains was obscured.[21] It is interesting to note that the undoped σ value and Raman frequency in Fig. 2 were fully recovered upon dedoping, suggesting that electron transport and the tangential modes are both insensitive to doping-induced structural disorder.

The continuous and reversible increases in σ and χ_P could be reconciled with homogeneous doping. On the other hand, the most natural explanation for the concentration-independent CESR linewidth and the XRD results is the inhomogeneous model presented above. If $N(E_F)$ increased continuously with doping, the CESR line should broaden monotonically due to increasing spin-orbit scattering with increasing K content, as observed in K-doped $(CH)_x$.[14] However, the CESR linewidth for K-doped SWNT is independent of K/C, the simplest interpretation being that $N(E_F)$

of the doped ''domains'' is constant, while the global K/C ratio simply reflects the volume fraction occupied by such domains. XRD reveals no long-range order within domains; as the domains grow in number or size, the crystalline fraction decreases. The ESR intensity is then proportional to the volume fraction of saturation-doped domains, which explains the quasilinear dependence of χ_P on K/C ratio. The spin relaxation rate is in turn constant, since $N(E_F)$ in the domains is independent of K/C.

In general, a two-phase model implies one or more first-order transitions vs chemical potential (or global concentration), as one well-defined phase grows at the expense of another. No evidence of such transitions is found in cyclic voltammetry (CV) or charge/discharge (CD) experiments,[7,8] which we attribute to the intrinsic disorder and nanoscopic length scale of the doped and undoped ''phases.'' Both kinds of domain consist of tubes with different diameters, chiralities, and lengths, such that there is no well-defined K-site binding energy. Furthermore, the small domain size is probably of the same order as the width of the ''domain walls,'' such that doped and undoped regions cannot be viewed as independent objects which merely exchange dopants with each other. We therefore expect a wide distribution of redox potentials such that redox peaks in CV and plateaus in CD are completely washed out.

In conclusion, we have detected CESR in doped SWNT and measured χ_P and the spin relaxation rate as a function of doping concentration for the first time. *In situ* conductivity, spin susceptibility, and Raman spectroscopy show continuous and reversible valence electron transfer from K to SWNT. *In situ* XRD shows an irreversible loss of crystallinity of the 2D rope lattice. We propose an inhomogeneous structural model for the doped phase to explain the XRD and the constant spin relaxation.

This work was supported by NSF Grant Nos. MRSEC-DMR96-32598 (A.S.C., J.E.F.), DMR97-30298 (N.M.N., A.J., J.E.F.), and by OTKA T 029150 (A.J.). Purified SWNT were graciously provided by A. G. Rinzler and R. E. Smalley. We thank B. Gibney and P. L. Dutton from the Johnson Research Foundation for the use of the EPR spectrometer; P. Bernier, A. A. Maarouf, P. K. Davies, E. J. Mele, and P. Petit for useful discussions; and L. Forro for sharing his unpublished result with us.

*Email: fischer@sol1.lrsm.upenn.edu

[1] R. S. Lee *et al.*, Nature (London) **388**, 255 (1997).
[2] R. S. Lee *et al.*, Phys. Rev. B **61**, 4526 (2000).
[3] A. M. Rao *et al.*, Nature (London) **388**, 257 (1997).
[4] G. Gao *et al.*, Phys. Rev. Lett. **80**, 5556 (1998).
[5] C. Bower *et al.*, Appl. Phys. A: Mater. Sci. Process. **67**, 47 (1998).
[6] S. Suzuki, C. Bower, and O. Zhou, Chem. Phys. Lett. **235**, 230 (1998).
[7] A. Claye *et al.*, J. Electrochem. Soc. (to be published).
[8] A. Claye and J. E. Fischer, Mol. Cryst. Liq. Cryst. Sci. Technol. Sect. A **340**, 743 (2000).
[9] J. E. Fischer, A. Claye, and R. S. Lee, Mol. Cryst. Liq. Cryst. Sci. Technol. Sect. A **340**, 737 (2000).
[10] L. Forró *et al.*, J. Phys. (France) **48**, 413 (1987).
[11] P. Petit *et al.*, Phys. Rev. B **56**, 9275 (1997).
[12] S. Bandow *et al.*, Appl. Phys. A: Mater. Sci. Process. **67**, 23 (1998).
[13] L. Forró (unpublished).
[14] C. Fite and P. Bernier, Phys. Rev. B **36**, 4574 (1987).
[15] A. G. Rinzler *et al.*, Appl. Phys. A: Mater. Sci. Process. **67**, 29 (1998).
[16] A. Thess *et al.*, Science **273**, 483 (1996).
[17] J. Amiell *et al.*, Mater. Sci. Eng. **31**, 243 (1977).
[18] M. F. Quinton, A. P. Legrand, and F. Beguin, Synth. Met. **14**, 179 (1986).
[19] G. Feher and A. F. Kip, Phys. Rev. **98**, 337 (1955).
[20] σ values are not corrected for porosity. Denser SWNT materials exhibit much higher σ; J. Hone *et al.*, Appl. Phys. Lett. (to be published).
[21] A. Claye *et al.* (unpublished).
[22] A. Janossy and P. Monod, Phys. Rev. Lett. **37**, 612 (1976).
[23] O. Chauvet *et al.*, Phys. Rev. B **53**, 13 996 (1996).
[24] A. A. Maarouf, C. L. Kane, and E. J. Mele, Phys. Rev. B **61**, 11 156 (2000).